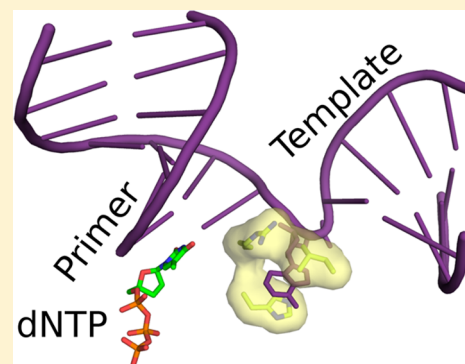


Structure–Function Studies of DNA Polymerase  $\lambda$ Katarzyna Bebenek,<sup>\*,†,‡</sup> Lars C. Pedersen,<sup>†</sup> and Thomas A. Kunkel<sup>†,‡</sup><sup>†</sup>Laboratory of Structural Biology and <sup>‡</sup>Laboratory of Molecular Genetics, National Institute of Environmental Health Sciences, National Institutes of Health, Research Triangle Park, North Carolina 27709, United States

**ABSTRACT:** DNA polymerase  $\lambda$  (pol  $\lambda$ ) functions in DNA repair with its main roles considered to be filling short gaps during repair of double-strand breaks by nonhomologous end joining and during base excision repair. As indicated by structural and biochemical studies over the past 10 years, pol  $\lambda$  shares many common properties with other family X siblings (pol  $\beta$ , pol  $\mu$ , and terminal deoxynucleotidyl transferase) but also has unique structural features that determine its specific functions. In this review, we consider how structural studies over the past decade furthered our understanding of the behavior and biological roles of pol  $\lambda$ .



Genomic DNA is constantly exposed to endogenous and exogenous damaging agents that threaten its integrity. To preserve the genetic information, multiple DNA transactions operate in cells, and most of these transactions involve the synthesis of new DNA by polymerases. Included among these polymerases are members of family X that are conserved in most organisms from bacteria to humans and are even encoded by viruses.<sup>1,2</sup> The X family contains four subfamilies,<sup>1</sup> DNA polymerases (pols)  $\beta$ ,  $\lambda$ , and  $\mu$  and terminal deoxynucleotidyl transferase (TdT). Only vertebrates encode polymerases from each subfamily,<sup>1</sup> suggesting that vertebrates require diversification and specialization of family X polymerase functions. Of the four eukaryotic family X members, pol  $\lambda$  is the most widely distributed across the biological kingdoms. Therefore, pol  $\lambda$  may be most similar to the common ancestor from which eukaryotic family X polymerases diversified.<sup>1</sup> Consistent with this idea, the properties of mammalian pol  $\lambda$  overlap with both of its template-dependent family X siblings, pols  $\beta$  and  $\mu$ . Thus, like pol  $\beta$ , pol  $\lambda$  participates in base excision repair (BER), and like pol  $\mu$ , it participates in repair of double-strand DNA breaks and has also been implicated in translesion DNA synthesis (TLS). In this review, we first consider the biological evidence of the participation of pol  $\lambda$  in these processes and then explore how our understanding of the biology has been advanced by structural studies of pol  $\lambda$  published over the past decade.

### ■ BASE EXCISION REPAIR

Base excision repair is the major pathway for repair of small DNA base lesions resulting from alkylation, oxidation, depurination/depyrimidination, and deamination. Two BER subpathways, the short patch and long patch BER, operate in eukaryotic cells. In contrast to long patch BER, with the repair tract of two or more nucleotides, short patch repair (Figure 1A) results in the replacement of a single damaged nucleotide, and DNA pol  $\beta$  is the primary polymerase involved in this process.<sup>3</sup>

The repair is initiated via the excision of the damaged base by a lesion-specific DNA glycosylase; this step is followed by AP-endonuclease cleavage of the sugar–phosphate backbone 5' of the AP site and replacement of the missing nucleotide by the polymerase. Finally, the lyase removes the 5'-deoxyribose phosphate (5'-dRP) group, allowing the ligase to seal the nick (Figure 1A). Pol  $\beta$  contributes two activities to the repair process, the polymerase catalytic activity and the dRP lyase activity, and seminal studies showed that the latter is rate-limiting for single-base BER by pol  $\beta$ .<sup>3</sup> Like pol  $\beta$ , pol  $\lambda$  has dRP lyase activity<sup>4</sup> and can substitute for pol  $\beta$  in reconstituted BER reactions *in vitro*.<sup>5</sup> Furthermore, it has been shown that pol  $\beta(-/-)$ , pol  $\lambda(-/-)$  double-knockout chicken DT40 cells and mouse embryonic fibroblasts<sup>6</sup> are significantly more sensitive than pol  $\beta(-/-)$  cells to oxidizing DNA-damaging agents and oxidizing and alkylating DNA-damaging agents, respectively. These results indicating a function in backup repair in pol  $\beta$  knockout cells support pol  $\lambda$ 's role in BER.

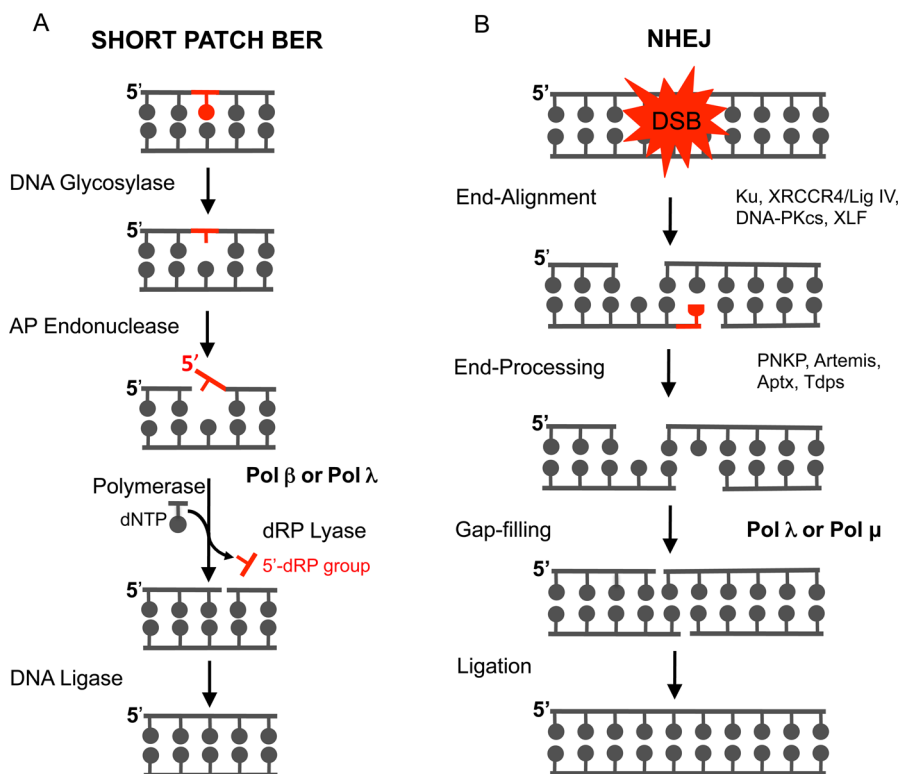
One of the most common DNA lesions repaired by BER is 8-oxo-7,8-dihydro-2'-deoxyguanosine (8-oxodG) induced by reactive oxygen species. Because of its dual coding potential (it can pair with both C and A), 8-oxodG is highly mutagenic generating GC to TA transversions. OGG1 glycosylase-dependent BER is the primary pathway responsible for removal of this lesion. In addition, the MutYH glycosylase-dependent BER pathway replaces the misincorporated dATP with dCTP opposite 8-oxodG. The 8-oxodG can then be removed by the OGG1 glycosylase.

Pol  $\lambda$  relatively efficiently incorporates both dATP and dCTP opposite 8-oxodG.<sup>7</sup> However, it has been shown that in the presence of replication protein A and PCNA, pol  $\lambda$  has a

Received: December 30, 2013

Revised: March 21, 2014

Published: April 10, 2014



**Figure 1.** DNA polymerase  $\lambda$  participates in BER and NHEJ. (A) Schematic representation of the short patch BER pathway. The nucleotide with the damaged base is colored red. 5'-dRP denotes the 5'-deoxyribose phosphate group. (B) Schematic representation of the NHEJ pathway. A damaged 5'-end nucleotide is colored red. Abbreviations: Ku, KU70–80 heterodimer; DNA-PKcs, catalytic subunit of DNA-dependent protein kinase; LigIV, ligase IV; PNKP, polynucleotide kinase phosphate; XLF, XRCC4-like factor; Aptx, aprataxin; Tdps, tyrosine phosphodiesterases.

stronger preference, compared to those of other cellular polymerases, for incorporation of C rather than A opposite template 8-oxodG.<sup>8</sup> Consistent with this property, pol  $\lambda$  has been implicated in long patch, MutYH-dependent BER.<sup>9</sup>

## ■ NONHOMOLOGOUS END JOINING

Nonhomologous end joining (NHEJ) is the main pathway in higher eukaryotes for repair of DNA double-strand breaks (DSBs). Chromosomal DSBs are the most severe type of DNA damage. They may be caused by exposure to ionizing radiation or chemicals such as DNA-cleaving chemotherapeutics. They may also result from indirect causes, including collapsed replication forks or aborted DNA repair reactions. Programmed chromosomal DSBs are intermediates in recombination associated with adaptive immune response [V(D)J and class switch recombination] and meiosis.<sup>10</sup> Damage-unrelated DSBs in neurons have been linked to physiological brain activity involving learning and memory.<sup>11</sup> Failure to repair a double-strand break may lead to cell death.

NHEJ is initiated by the alignment of broken, largely incompatible, and often damaged DNA ends using limited base pairing (Figure 1B). This process involves the key end-joining factors, the Ku70–80 heterodimer, XRCC4, ligase IV, DNA-dependent protein kinase (DNA-PK), and XLF/Cernunos.<sup>10,12–14</sup> Moreover, additional factors such as polynucleotide kinase phosphate (PNKP), aprataxin (Aptx), and tyrosine phosphodiesterases (Tdps) are usually required to process damaged DNA ends (reviewed in refs 10, 13, and 14 and references cited therein). Duplexes generated by alignment of the broken DNA ends often contain small gaps that need to be filled by a DNA polymerase, and family X members have been

implicated in this function. While the role of TdT in DSB repair is restricted to V(D)J recombination, pol  $\lambda$  and pol  $\mu$  function both in V(D)J recombination and in general NHEJ. V(D)J recombination is a specialized form of end joining that occurs in cells of the immune system at the antigen receptor gene loci and is responsible for the diversification of the antigen recognition site. Pol  $\lambda$ 's role in V(D)J recombination is in heavy chain gene rearrangement at a step preceding the action of TdT,<sup>15</sup> although lack of pol  $\lambda$  activity does not impair B-cell development. In contrast, pol  $\mu$  promotes the accuracy of light chain gene rearrangement. Its absence results in excessive deletions at the light chain junctions causing B-cell deficiency.<sup>16</sup> These results indicate that the functions of pol  $\lambda$  and pol  $\mu$  in V(D)J recombination clearly do not overlap.

Pol  $\lambda$  has been shown to participate in NHEJ reactions in HeLa cell extracts.<sup>17</sup> In addition, in the extract-based end joining reaction, pol  $\lambda$  is able to extend an 8-oxodG-terminated primer.<sup>18</sup> This ability is consistent with a role in joining of damaged DNA ends. Pol  $\lambda$  can also perform gap filling synthesis in reconstituted NHEJ reactions *in vitro*.<sup>19,20</sup> Furthermore, studies with cultured cells support pol  $\lambda$ 's involvement in NHEJ but suggest some redundancy in the function of pol  $\lambda$  and pol  $\mu$ .<sup>15,21</sup> These observations are consistent with results showing that pol  $\mu$  can utilize substrates similar to those of pol  $\lambda$  during *in vitro* NHEJ reactions.

## ■ TRANSLESION SYNTHESIS


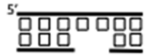
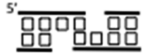
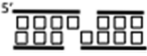
Translesion synthesis is a damage tolerance system in which specialized polymerases substitute for replicative polymerases in copying across DNA lesions during replication.<sup>22</sup> It has been suggested that pol  $\lambda$  is involved in translesion synthesis of

abasic sites<sup>23,24</sup> and 8-oxodG lesions, and that DNA polymerase  $\delta$ -interacting protein 2 (PolDIP2) stimulates the 8-oxodG bypass activity of pol  $\lambda$ .<sup>25</sup> Pol  $\lambda$  has also been shown to perform gap filling opposite thymine glycol<sup>26</sup> and a benzo[*a*]pyrene-derived DNA adduct.<sup>27</sup>

## BIOCHEMICAL PROPERTIES AND DOMAIN ORGANIZATION OF POL $\lambda$

Like its family X siblings, pol  $\lambda$  is a single-subunit, monomeric enzyme with limited processivity and no intrinsic 3'  $\rightarrow$  5' exonucleolytic activity to proofread errors.<sup>28–30</sup> Its base substitution error rate (Table 1) is similar to that of pol  $\beta$ .

**Table 1. Biochemical Properties of Pol  $\lambda$ <sup>b</sup>**

Activities	
Lyase	+
Polymerase	+
- Catalytic efficiency ( $\mu\text{M}^{-1}\text{s}^{-1}$ )	0.36–1.4
- Processivity	
Open template	1
Gap substrate	1–5
- Fidelity (error rate $\times 10^{-4}$ )	
Base substitutions	9
1 nucleotide deletions	45
Exonuclease 3' $\rightarrow$ 5'	-
Substrates in Repair	
	Yes BER
	Yes BER/NHEJ <sup>a</sup>
	Yes NHEJ
	No

<sup>a</sup>Pol  $\lambda$  may fill in two-nucleotide gaps in the context of BER and upon alignment of broken DNA ends during NHEJ. <sup>b</sup>Catalytic efficiency values taken from refs 32 and 86, processivity values taken from ref 32, and fidelity values taken from ref 31.

However, pol  $\lambda$  generates single-nucleotide deletions at an exceptionally high rate (Table 1), higher even than that of the Y family polymerases.<sup>31</sup> Pol  $\lambda$  has a high affinity for dNTPs,<sup>32</sup> which may allow it to conduct synthesis when the concentration of precursors in the cell is low, e.g., outside S-phase in cycling cells or in quiescent cells.

With 575 amino acids and a molecular mass of 65 kDa, pol  $\lambda$  is the largest of the four human family X polymerases.<sup>28,29,32</sup> Its catalytic core (residues 252–575) comprises a C-terminal polymerase domain containing the fingers, palm (containing the three catalytic aspartates), and thumb subdomains, and an N-terminal 8 kDa domain (Figure 2A,B). In addition to the catalytic core, pol  $\lambda$  has a single N-terminal breast cancer

carboxy-terminal (BRCT) domain separated from the catalytic core by a serine-proline-rich domain (Ser/Pro) (Figure 2A,C).

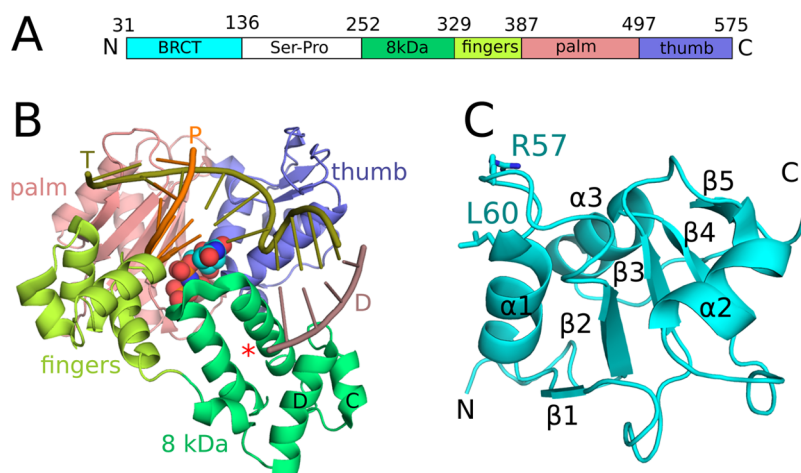
The amino acid sequence of Pol  $\lambda$ 's catalytic core is 34 and 30% identical with those of pol  $\beta$  and the catalytic core of pol  $\mu$ , respectively. Its X-ray crystal structure in complex with DNA containing a one-nucleotide gap and an incoming nucleoside triphosphate<sup>33</sup> reveals an overall protein fold common to pol  $\beta$ , pol  $\mu$ , and TdT (Figure 2B), with the same secondary structure elements. As observed in the structures of pols  $\beta$  and  $\mu$ ,<sup>34,35</sup> pol  $\lambda$  also binds both sides of the gap, imposing a 90° bend in the DNA to expose the primer terminus and the templating nucleotide<sup>36</sup> (Figure 2B). The polymerase domain binds the 3'-end of the gap, interacting with the primer-terminal base pair and the upstream duplex DNA. The 8 kDa domain interacts with the 5'-end of the gap, with binding facilitated by the 5'-phosphate.<sup>32</sup>

## BRCT DOMAIN

The involvement of pol  $\lambda$  in NHEJ of broken DNA ends depends on its N-terminal BRCT domain, which is required for interactions with two essential NHEJ complexes, Ku and XRCC4-ligase IV.<sup>17,19,20,37–39</sup> The BRCT domain is not critical for polymerase catalytic activity, as indicated by the ability of a pol  $\lambda$  variant lacking the BRCT domain to perform gap filling synthesis *in vitro*. However, consistent with the role of the BRCT domain in mediating interactions with the end-joining factors, the variant fails to perform synthesis in the context of NHEJ. The amino acid sequence of the pol  $\lambda$  BRCT domain is only 23 and 20% identical with those of the BRCT domains of pol  $\mu$  and TdT, respectively. Despite this relatively low level of sequence conservation, the nuclear magnetic resonance solution structure of the pol  $\lambda$  BRCT domain<sup>40</sup> shows an overall fold and spatial arrangement of secondary structural elements (five short  $\beta$ -strands that constitute the core of the domain, flanked by  $\alpha$ -helices 1–3) that is observed in the structures of the BRCT domains of pol  $\mu$  and TdT.<sup>40,41</sup> In the BRCT domains of all three polymerases,  $\alpha$ -helix 1 is pivotal to interactions with the end-joining factors, with structural variations in the interaction surface observed among the three.<sup>40</sup> Three conserved residues of  $\alpha$ -helix 1, an N-terminal arginine and two solvent-exposed hydrophobic residues, are critical for binding of pol  $\mu$  and TdT to Ku and XRCC4-ligase IV. Only two of these residues are conserved in pol  $\lambda$ , the N-terminal Arg57 and Leu60, which replaces a phenylalanine in pol  $\mu$  and TdT. Substitutions at either of these two pol  $\lambda$  residues impair complex formation with the end-joining factors and activity in NHEJ.<sup>40</sup> These structural differences between the BRCT domains of pol  $\lambda$  and its siblings suggest functional differences in the formation of the complex with the NHEJ partners.

## SERINE-PROLINE-RICH REGION

The serine-proline-rich region is present only in pol  $\lambda$  and its *Saccharomyces cerevisiae* homologue, pol IV. This region was originally suggested to be a target for post-translational modification.<sup>28</sup> More recent studies have shown that several serine residues in this region are indeed modified by phosphorylation, thereby protecting pol  $\lambda$  from ubiquitin-dependent degradation and modulating its activity in the MutYH glycosylase-dependent BER pathway.<sup>42</sup> This region has also been suggested to play a role in modulating the fidelity of pol  $\lambda$ .<sup>43</sup>



**Figure 2.** Domain organization of polymerase  $\lambda$ . (A) Schematic representation of domains in pol  $\lambda$ . (B) Crystal structure of the ternary complex of the catalytic domains of polymerase  $\lambda$  with bound one-nucleotide gapped DNA and an incoming nucleotide (PDB entry 2PFO). The 8 kDa DRP lyase domain, fingers, palm, and thumb subdomains are colored lime green, lemon, salmon, and slate, respectively. The DNA templating strand (T) is colored olive, the primer strand (P) orange, and the downstream strand (D) violet. The position of the 5'-phosphate is marked with a red asterisk. A space-filling model of the incoming nucleotide is colored cyan. (C) Nuclear magnetic resonance solution structure of the BRCT domain of pol  $\lambda$ . Secondary structural elements as well as potential protein-interacting residues Arg57 and Leu60 are labeled. All structural figures were created with PyMol from Schrödinger (<http://www.pymol.org>).

## ■ THE 8 KDA DOMAIN

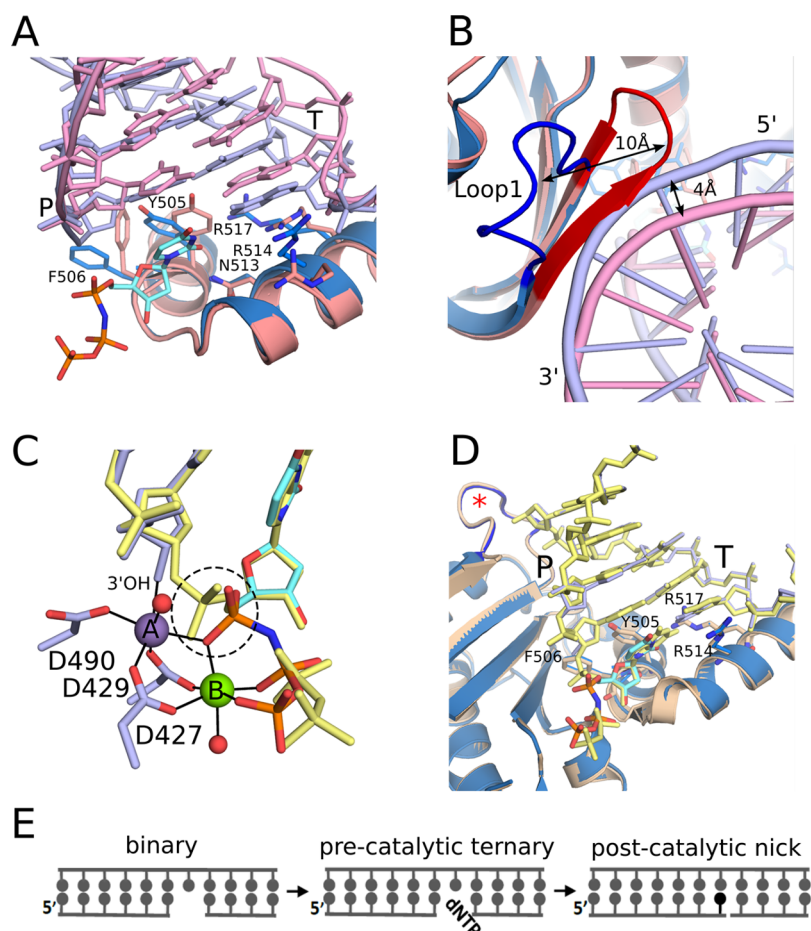
The 8 kDa domain (Figure 2A,B) is a characteristic feature of most X family polymerases. In a manner similar to what was originally reported for pol  $\beta$ ,<sup>44</sup> the 8 kDa domain of pol  $\lambda$  binds to the 5'-end of a DNA gap, allowing the enzyme to bridge both ends of the gap. The phosphate moiety is bound in a positively charged pocket formed by pol  $\lambda$  residues Arg275, Arg308, and Lys312. The binding of the 5'-phosphate stimulates the gap filling activity of pol  $\lambda$  and increases its processivity. A helix-hairpin-helix motif (HhH) in the 8 kDa domain also contributes to DNA binding through interactions with the DNA backbone on the downstream side of the gapped substrate. It spans  $\alpha$ -helices C and D (Figure 2B) and contains a characteristic hairpin loop sequence G $\phi$ G ( $\phi$  represents a hydrophobic residue) that is conserved in HhH motifs of other DNA binding proteins. The 8 kDa domain also harbors one of the two catalytic activities of pol  $\lambda$ 's catalytic core, the DRP lyase. As with pol  $\beta$ , the lyase activity of pol  $\lambda$  is proposed to proceed through a  $\beta$ -elimination mechanism with formation of a Schiff base intermediate.<sup>45</sup> The main catalytic nucleophile is Lys312,<sup>4</sup> located in the pocket that binds the 5'-phosphate end of the DNA gap.

Pol  $\lambda$  also has a short sequence preceding the 8 kDa domain termed the "brooch".<sup>46</sup> In human pol  $\lambda$ , the brooch contains residues Trp239–Gln243 and is conserved in other members of the pol  $\lambda$  subfamily. Similar sequences are also present in pol  $\mu$  and TdT, but not in pol  $\beta$ . The residues of the brooch mediate interactions between the 8 kDa domain and the thumb subdomain, leading to the suggestion that the function of the brooch is to facilitate enzyme–substrate interactions during synthesis to fill gaps longer than one nucleotide.<sup>46</sup>

## ■ CATALYTIC MECHANISM FOR CORRECT INCORPORATION

Although DNA polymerases from different families have distinctive subunit compositions, biochemical properties, and biological functions, they all catalyze the same basic nucleotidyl transfer reaction.<sup>47</sup> This involves incorporating of a nucleoside

monophosphate onto a 3'-end of a DNA primer and releasing a pyrophosphate, in a reaction requiring activation by (at least) two divalent metal ions. Studies of polymerases from different families show that assembly of the active site for polymerization involves multiple conformational changes triggered by binding of the incoming dNTP. Some of these conformational changes are believed to function as kinetic checkpoints to discriminate against incorporation of incorrect nucleotides.<sup>48</sup> In many polymerases, including members of families A and B as well as pol  $\beta$ , dNTP binding induces large subdomain motions, wherein the fingers and thumb subdomains relocate relative to each other, leading to a catalytically competent, "closed" conformation.<sup>34,49,50</sup> Interestingly, pol  $\lambda$  does not undergo this large "open to closed" transition.<sup>33</sup> Rather, a comparison of the X-ray crystal structures of pol  $\lambda$  pre- and postcatalytic complexes (Figure 3) indicates that the polymerase remains closed throughout the catalytic cycle. Nonetheless, binding of the incoming dNTP does induce a shift of the template strand to bring the templating nucleotide into the active site. Concurrently, loop1 between  $\beta$ -strands 3 and 4 in the palm subdomain relocates to allow the template strand to assume its active conformation (Figure 3A,B). In addition, several amino acid side chains reposition to form the nascent base pair binding pocket and establish interactions with the DNA minor groove (Figure 3A) that are important for base selectivity and catalysis. For example, in the minor groove of duplex DNA, the positions of the O2 atoms of pyrimidines and the N3 atoms of purines (both hydrogen bond acceptors) are almost identical for all four correct Watson–Crick base pairs, but not for mismatches. DNA polymerases are thought to check for correct base pair geometry using side chain interactions that probe the position of the minor groove hydrogen bond acceptors (reviewed in ref 51, and see references cited therein). In pol  $\lambda$ , this role appears to be played by Tyr505 and Arg517, which together with Phe506 are repositioned in the minor groove of DNA upon binding of a correct dNTP. Once in their active conformation, the side chains of Tyr505 and Arg517 interact with the minor groove of the primer-terminal base and its template counterpart, respectively. Arg517 may also interact



**Figure 3.** Conformational changes during catalysis. (A) Superimposition of the binary structure of pol  $\lambda$  (salmon) with a one-nucleotide gap DNA substrate (pink) onto that of the pre-catalytic ternary complex (royal blue) with a one-nucleotide gap DNA substrate (light blue) and an incoming nonhydrolyzable nucleotide, dUMPNPP, 2'-deoxyuridine 5'-[( $\alpha,\beta$ )-imido]triphosphate (cyan) (PDB entries 1XSL and 2PFO, respectively). (B) Different orientation of the structures from panel A (blue for ternary complex and red for binary) showing loop 1 and DNA template movement upon binding the nucleotide. (C) Superimposition of the active sites of the post-catalytic complex (DNA colored yellow) on that of the ternary, pre-catalytic complex (colored as in panels A and B) (PDB entries 1XSP and 2PFO, respectively). The catalytic metals are colored purple for metal A and green for metal B, with the metal coordination displayed as solid black lines. The phosphate of the incoming nucleotide that undergoes a stereochemical inversion upon attack by the 3'-OH of the primer is circled. (D) Global view of the structures in panel C with the protein from the post-catalytic complex colored wheat. Loop 1 is marked with a red asterisk. (E) Schematic of the DNA present in the crystal structures of the binary, ternary, and post-catalytic nick complexes.

with the minor groove atoms of the templating base, while yet another residue, Asn513, interacts with O2 or N3 of the incoming nucleotide. Assembly of the active site also involves relocation of Arg514 to a position that stabilizes the templating nucleotide through stacking interactions with the base. Compared to minor groove interactions of polymerases in families A and B extending several base pairs upstream of the primer terminus, existing structures suggest that pol  $\lambda$  requires correct Watson–Crick geometry only for the two base pairs directly involved in catalysis, i.e., the primer-terminal base pair and the newly forming base pair.

Structures of pol  $\lambda$  pre- and post-catalytic complexes (Figure 3A–E) combined with quantum mechanics/molecular mechanics simulations<sup>33,52,53</sup> strongly support the two-metal-ion-catalyzed phosphoryl transfer mechanism<sup>54</sup> requiring two divalent metal ions. While  $Mg^{2+}$  is likely to be the metal ion most often used by polymerases *in vivo*, it is well-known that  $Mn^{2+}$  can substitute for  $Mg^{2+}$  *in vitro*, and it has been proposed that some DNA polymerases, including pol  $\lambda$ , may use  $Mn^{2+}$  as the preferred activating metal ion *in vivo*.<sup>55</sup> The involvement of

a third metal ion in the catalytic reaction was recently reported for pol  $\eta$  and pol  $\beta$ <sup>56,57</sup> (for related information on these two polymerases, please refer to refs 58 and 59). The possible involvement of a third metal in catalysis by pol  $\lambda$  has yet to be investigated. In the structure of the pol  $\lambda$  pre-catalytic complex with a one-nucleotide gap DNA and a correct nonhydrolyzable nucleotide, all atoms required for catalysis are present at the active site (Figure 3C). The two catalytic metals (A and B) coordinate with the three active site aspartate residues (Asp490, Asp427, and Asp429), O3' of the primer, and the incoming nucleoside triphosphate. The nonbridging oxygens of the triphosphate moiety of the incoming dNTP coordinate metal B. Coordination of metal A results in a conformational change in the primer-terminal ribose and is believed to facilitate the transfer of the proton from the nucleophilic O3' to the proposed proton acceptor, Asp490.<sup>53</sup> In the structure of the post-catalytic complex containing the newly incorporated nucleotide bound at the active site, the conformation of the enzyme and the DNA is nearly identical to that of the pre-catalytic complex (Figure 3D). The only apparent changes

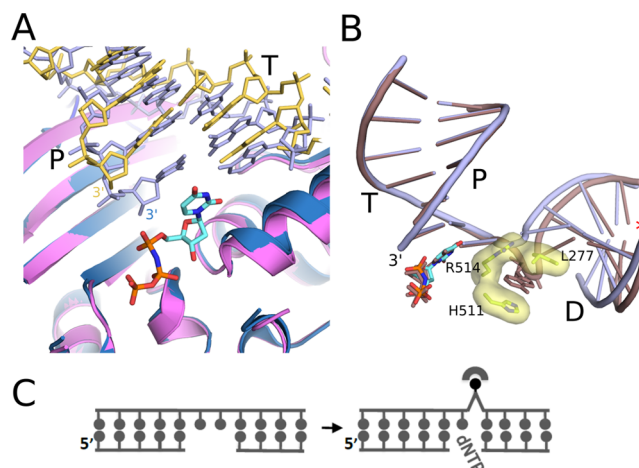
in the postcatalytic complex are the stereochemical inversion of the  $\alpha$ -phosphate group and the breakage and formation of a new phosphorus–oxygen bond (Figure 3C). These structures suggest a catalytic path that is in agreement with the reaction mechanism originally proposed for pol  $\beta$ .<sup>60</sup> This reaction involves an in-line attack of the deprotonated O3' on the  $\alpha$ -phosphate of the incoming dNTP, leading to a trigonal-bipyramidal pentacoordinated transition state and resulting in the inversion of the stereochemistry of the  $\alpha$ -phosphate. Release of the pyrophosphate is the final step in single-nucleotide gap filling synthesis.

### ■ TEMPLATE SCRUNCHING FACILITATES FILLING GAPS LONGER THAN ONE NUCLEOTIDE

NHEJ or long patch BER involves filling gaps longer than one nucleotide. Biochemical data suggest that when filling a gap of up to five nucleotides, pol  $\lambda$  simultaneously interacts with both ends of the gap. As discussed below, such a mode of interaction requires that the polymerase is able to accommodate the as-yet uncopied template nucleotides while engaging both ends of the gap in a catalytically competent manner.

When pol  $\lambda$  binds to a one-nucleotide gap-containing DNA, despite the absence of an incoming dNTP, the 3'-end of the gap is located adjacent to the nucleotide binding site, while the 5'-end is bound by the 8 kDa domain in a manner similar to that depicted in Figure 2B. Except for some adjustments in the conformation of the ribose and the positioning of the 3'-OH, the general location of the 3'-terminal nucleotide and the position of the primer strand do not change upon binding of the incoming dNTP (Figure 3A). This is not the case when the gap is longer. In the structure of the pol  $\lambda$  binary complex with a two-nucleotide gap DNA, the 8 kDa domain binds the 5'-end of the gap, as in the complex with the one-nucleotide gap. However, the 3'-primer-terminal nucleotide is not productively engaged and is shifted upstream from the position adjacent to the dNTP binding site<sup>36</sup> (Figure 4A). This structure suggests that DNA binding by pol  $\lambda$  is directed predominantly by the 8 kDa domain, which anchors the polymerase at the 5'-end regardless of the conformation of the 3'-end. When the incoming dNTP binds, the 3'-primer-terminal nucleotide as well as amino acid residues that form the active site and the nascent base pair binding pocket assume an identical position as observed in the structure of the ternary complex with a one-nucleotide gap. The incoming dNTP is bound opposite the 3'-template nucleotide of the gap, which is located at the active site (Figure 4B). Though the gap is one nucleotide longer, the distance between the 3'-end of the gap and the 5'-end bound by the 8 kDa domain is the same as in the one-nucleotide gap structure. This is possible because the template strand is scrunched, such that the 5'-template nucleotide of the gap is in an extrahelical conformation.<sup>61</sup> The extrahelical nucleotide is bound in a pocket created by three amino acid residues, Leu277, His511, and Arg514, with minimal distortion of the DNA geometry (Figure 4B,C). The three residues that form the scrunching pocket are conserved in pol  $\lambda$  orthologs but not in other pol X polymerases from vertebrate cells. This suggests that relative to other family X members, pol  $\lambda$  has a unique way of binding a gap longer than one nucleotide, a property that may be relevant to its role in DNA repair *in vivo*.

Molecular dynamics simulations of pol  $\lambda$  ternary complexes indicate that even when the gap is longer (containing three or four nucleotides) the template strand assumes a scrunched conformation in which the nucleotide immediately 5' to the



**Figure 4.** Filling of a two-nucleotide gap. (A) Superimposition of a binary structure of pol  $\lambda$  (pink) bound to a two-nucleotide gap substrate (yellow) superimposed with the ternary one-nucleotide gap complex (colored as in Figure 3) (PDB entries 1RZT and 2PFO, respectively). (B) Superimposition of the two-nucleotide gap precatalytic ternary complex (DNA colored brown, scrunch pocket residues colored yellow, and the incoming nucleotide colored brown) with the one-nucleotide gap precatalytic ternary complex colored as in panel A. The red asterisk denotes the 5'-phosphate on the downstream DNA strand (PDB entries 3HWT and 2PFO, respectively). (C) Schematic of DNA present in the binary and ternary two-nucleotide gap complexes.

templating nucleotide is preferentially bound in the pocket.<sup>61</sup> Furthermore, the polymerase can accommodate the additional 5'-uncopied template nucleotides while maintaining the same conformation as observed in the structure. These models are consistent with biochemical data suggesting that, when filling a gap of up to five nucleotides, pol  $\lambda$  engages both ends of the gap.<sup>32</sup>

The X-ray crystal structure of a ternary complex of a pol  $\lambda$  mutant with alanine substitutions at all three residues of the binding pocket suggests that the binding of the extrahelical nucleotide in the pocket stabilizes the scrunched conformation.<sup>61</sup> Failure to stabilize the scrunched conformation, as in the case of the triple mutant, decreases the processivity of gap filling synthesis by causing the enzyme to dissociate from the DNA more readily and/or to translocate less efficiently. It also reduces the efficiency of end joining in NHEJ reactions that require filling of a two-nucleotide gap,<sup>61</sup> indicating that the ability to bind the uncopied template nucleotide in the scrunching pocket is important in repair-related synthesis.

### ■ CATALYSIS USING MISALIGNED SUBSTRATES

All DNA polymerases occasionally introduce errors during DNA synthesis, usually generating base substitutions at a rate higher than the rate of insertion–deletion (indels) errors.<sup>62</sup> Pol  $\lambda$  is unusual because its exceptionally high rate of single-nucleotide deletions exceeds its rate of base substitutions.<sup>31</sup> Typically, DNA polymerases introduce indels more frequently in repetitive sequences than at noniterated nucleotides.<sup>63,64</sup> In addition, on the basis of results for polymerases from different families, including pol  $\beta$ , the rate of single-nucleotide deletions increases as a function of the polymeric run length.<sup>62</sup> These results are in agreement with the explanation proposed by Streisinger for insertions and deletions caused by DNA strand slippage during DNA synthesis.<sup>65</sup> Slippage in repetitive

sequence allows the formation of a misaligned template-primer in which the unpaired base within the duplex DNA upstream of the active site may be stabilized by one or more correct base pairs.<sup>65,66</sup> Furthermore, the longer the repeated sequence, the larger the number of correct base pairs between the unpaired nucleotide and the primer terminus. This, in turn, results in increased stability of the misaligned substrate, allowing for more efficient extension by the polymerase.

Similar to other polymerases, pol  $\lambda$  generates single-nucleotide deletions more frequently in short homopolymeric repeats than in noniterated sequences. However, unlike the case with other polymerases, the rate of these deletions does not increase further when the length of the nucleotide repeats increases from two to three (or more). This specificity, together with its relatively high noniterated nucleotide deletion rate, suggests that pol  $\lambda$  can efficiently utilize a misaligned primer-template stabilized by as few as one correct base pair. This ability is likely related to pol  $\lambda$ 's minimal interactions with the template strand, as well as the DNA minor groove. The latter interactions, used by the polymerase to probe for correct Watson–Crick base pair geometry, are limited in pol  $\lambda$  to the primer terminus and the newly formed base pairs. Consistent with this observation are structures of pre- and postcatalytic complexes of pol  $\lambda$  with a gapped DNA substrate containing an extra, unpaired template nucleotide upstream of the primer-terminal base pair, mimicking a misaligned single-nucleotide deletion intermediate (Figure 5A,B).<sup>67</sup> Superposition of the precatalytic misalignment-containing complex structure with

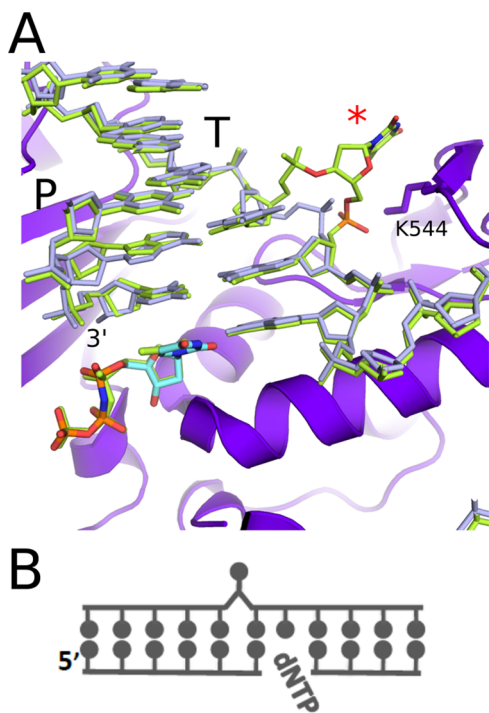
that of an equivalent complex with a correctly aligned one-nucleotide gap DNA indicates that the only apparent difference between the two is the presence of the extra nucleotide and a slight repositioning of the phosphate 5' to the extra base in the former (Figure 5A). The unpaired nucleotide is positioned immediately upstream from the primer-terminal base pair in an extrahelical conformation (Figure 5A,B). It is stabilized by interactions with a loop in the thumb subdomain (residues 540–548), specifically by interaction of Lys544 with the 5'-neighboring phosphate. A similar type of interaction, between a lysine residue and the 5'-phosphate next to the extrahelical base, has been described for base-flipping enzymes.<sup>68,69</sup> The fact that among family X enzymes the loop in the thumb is conserved only in pol  $\lambda$  may be in part responsible for its unique mutational specificity.

The good agreement between the two structures indicates that pol  $\lambda$  bound to the misaligned substrate is trapped in a conformation consistent with catalysis. Consequently, similar to the pre- and postcatalytic complexes with the correctly aligned substrates, the only major differences between the pre- and postcatalytic complexes with the misalignment are the making and breaking of the phosphorus–oxygen bond and the inversion of the stereochemistry of the  $\alpha$ -phosphate. These structures, corresponding to steps in the path to a single-nucleotide deletion, provide mechanistic insights into the basis of the mutational specificity of pol  $\lambda$ . They also indicate that pol  $\lambda$  can tolerate distortion of the DNA substrate immediately upstream of the active site.

Thus, the deletion signature of pol  $\lambda$  and the structures of complexes with single-nucleotide deletion intermediates, showing that pol  $\lambda$  can tolerate distortion of the primer-template immediately upstream of the active site, reveal properties of the enzyme that are ideal for a role in NHEJ of DNA ends containing damaged or mismatched nucleotides.

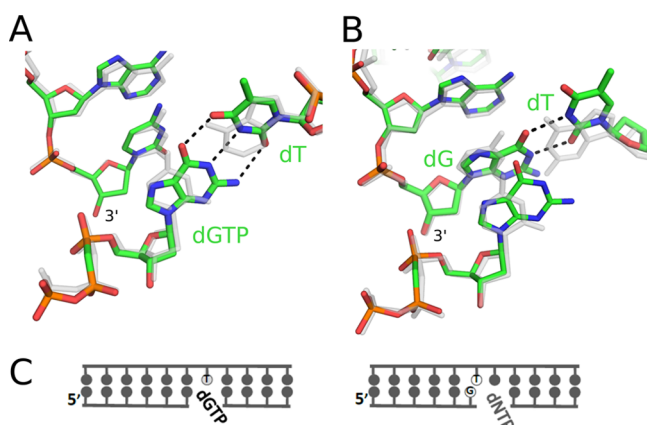
## ■ CATALYTIC MECHANISM FOR MISINCORPORATION

DNA polymerases are believed to use the prechemistry conformational changes as fidelity checkpoints, for exclusion of incorrect nucleotides.<sup>48,64</sup> Despite the fact that pol  $\lambda$  remains in a closed conformation throughout the catalytic cycle and does not undergo extensive conformational changes upon dNTP binding, it discriminates against incorrect nucleotides relatively efficiently. Its base substitution error rate is only 4-fold higher than that of pol  $\beta$ .<sup>31</sup> This is a relatively modest difference compared to its 30-fold higher single-nucleotide deletion rate. The base selectivity of pol  $\lambda$  is modulated by loop 1, located upstream of the active site in the palm subdomain. This loop is absent in pol  $\beta$ , but a longer loop 1 is present in pol  $\mu$  and TdT and has been implicated in DNA substrate selectivity.<sup>20</sup> Loop 1 of pol  $\lambda$  relocates in response to dNTP binding to allow the templating nucleotide to enter the active site (Figure 3B). Alteration of loop 1 in pol  $\lambda$  via removal of five residues and replacement of four residues with the corresponding sequence from pol  $\beta$  does not reduce the catalytic activity or alter the geometry of the active site for correct incorporation. However, consistent with the elimination of one or more kinetic checkpoints that prevent misincorporation, the base substitution error rate of the loop deletion mutant increases for all 12 mispairs and its sugar selectivity decreases.<sup>70,71</sup> These data support the idea that elimination of this fidelity checkpoint, by deletion of loop 1, lowers the energy barrier for establishing active site geometry consistent with catalysis.



**Figure 5.** Creating a single-nucleotide deletion. (A) Crystal structure of a precatalytic ternary complex of pol  $\lambda$  (protein colored violet and DNA and incoming nucleotide colored light green) representing creation of a single-nucleotide deletion, superimposed with the DNA and incoming nucleotide (light blue and cyan, respectively) from the ternary complex of a one-nucleotide gap structure (PDB entries 2BCV and 2PFO, respectively). The extrahelical nucleotide on the template strand is marked with a red asterisk. (B) Schematic of the single-nucleotide deletion intermediate in the structure.

Because of its properties, the loop 1 deletion variant proved to be a good model for structural studies of nucleotide misincorporation. The structure of the loop 1 variant in a ternary, precatalytic complex (Figure 6A,C) with an incoming

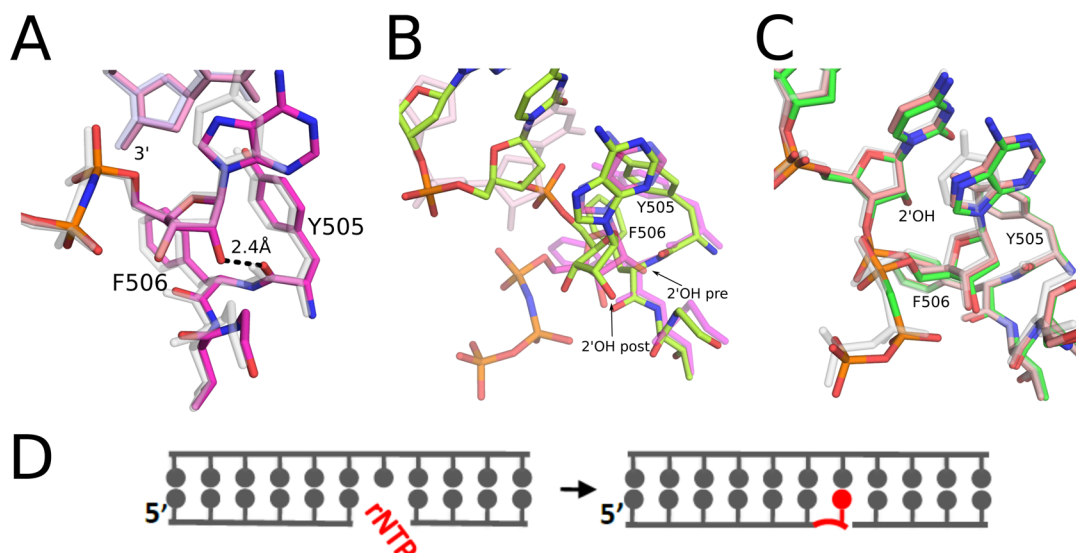


**Figure 6.** Mispairing in the active site of polymerase  $\lambda$ . (A) Ternary complex structure of an incoming dGMPCCP 2'-deoxyguanosine-5'-[( $\alpha,\beta$ )-methylene]triphosphate analogue opposite a templating dT (green) superimposed with a ternary complex with the correct incoming dNTP shown in transparent gray (PDB entries 3PMN and 2PFO, respectively). Potential hydrogen bonds are displayed with black dashed lines. (B) Ternary complex structure of a G-T mispair at the primer terminus with an incoming dGMPCCP (green) superimposed with a ternary complex with correctly paired DNA shown in transparent gray (PDB entries 3PNC and 2PFO, respectively). (C) Schematic of the DNA with a G-T mispair at the nascent base pair binding site (left) and at the end of the primer terminus (right).

nonhydrolyzable dGTP homologue opposite a template T demonstrates that the nascent dGTP-T mismatch at the

polymerase active site maintains Watson-Crick geometry (Figure 6A).<sup>72</sup> This result supports Watson and Crick's suggestion, 60 years ago, that spontaneous base substitutions could originate from mispairs having correct base pair geometry.<sup>73</sup> The original hypothesis implicated the involvement of bases in rare tautomeric forms, whereas subsequent studies suggested that ionized bases also could form mispairs with correct Watson-Crick geometry.<sup>74</sup> It remains to be determined which of the two forms, rare tautomers or ionized bases, contribute to the dGTP-T mismatch at the active site in the pol  $\lambda$  structure.<sup>72</sup> Nevertheless, consistent with the correct Watson-Crick geometry of the mispair, there is no distortion at the active site. All atoms needed for catalysis are present, and their positions overlay well with those in the structure of a precatalytic complex with a correct base pair<sup>72</sup> (Figure 6A). This suggests that the catalytic mechanism for insertion of an incorrect nucleotide can be the same as for the correct one. A C-A mispair with a correct Watson-Crick geometry was observed in the structure of a precatalytic complex of *Bacillus stearothermophilus* polymerase I large fragment (BF).<sup>75</sup> This C-A mispair is reported to form with rare tautomers and not ionized bases.

The following step on the path to a stable misincorporation is the extension of the mispaired primer terminus. The second mismatch-containing structure of the pol  $\lambda$  variant precatalytic complex indicates that upon misincorporation the now primer-terminal G-T mispair assumes a wobble conformation wherein the template T is shifted toward the major groove (Figure 6B,C). This distortion, however, does not affect the conformation of the nascent base pair or the catalytically competent geometry at the active site. These two structures visualize how a G-T mispair can be stably incorporated by pol  $\lambda$  and suggest why errors resulting from misincorporation of



**Figure 7.** Ribonucleotide incorporation by pol  $\lambda$ . (A) Precatalytic ternary complex with an incoming nonhydrolyzable ribonucleotide, rAMPNPP, adenosine 5'-[( $\alpha,\beta$ )-imido]triphosphate (magenta), superimposed with the ternary complex with an incoming deoxyribonucleotide (transparent gray) (PDB entries 3UPQ and 2PFO, respectively). The hydrogen bond between the 2'-OH and the carbonyl of Y505 is displayed as a dashed line. (B) Superimposition of the ternary complex with an incoming ribonucleotide (transparent magenta) with the postcatalytic complex with the newly incorporated rNMP (lemon) (PDB entries 3UPQ and 3UQ0, respectively). (C) Superimposition of precatalytic (green) and postcatalytic (peach) complexes with a ribonucleotide at the primer terminus. Also superimposed is the structure of the precatalytic ternary complex with the incoming deoxyribonucleotide (transparent gray) (PDB entries 4FO6, 3UQ2, and 2PFO, respectively). (D) Schematic of DNA in the pre- and postcatalytic structures with a ribonucleotide at the incoming position.



dGTP opposite T are the most frequent base substitutions generated by this polymerase.<sup>70</sup>

## ■ CATALYTIC MECHANISM FOR RIBONUCLEOTIDE INCORPORATION

rNTPs appear to be the most common noncanonical nucleotides incorporated into the genome. Recent studies indicate that large numbers of rNTPs are incorporated by high-fidelity polymerases during DNA replication.<sup>76,77</sup> It is believed that the probability of incidental rNTP incorporation is increased because of the higher cellular levels (10–200-fold) of rNTPs relative to dNTPs.<sup>76</sup>

Discrimination against rNTPs by family X members varies by several orders of magnitude depending on the enzyme, with TdT and pol  $\mu$  discriminating much less efficiently<sup>78–80</sup> than pols  $\lambda$  and  $\beta$ .<sup>81,82</sup> In fact it was suggested that TdT and pol  $\mu$  may use rNTPs as legitimate substrates during repair of DSBs by NHEJ in nonproliferating cells when the levels of rNTPs are high relative to the levels of dNTPs.<sup>78–80,83</sup> The relatively high sugar selectivity of pols  $\lambda$  and  $\beta$  is nevertheless lower than that of most replicative polymerases from families A and B. Therefore, pol  $\lambda$  and  $\beta$  could also occasionally incorporate rNTPs during repair synthesis. The structural characterization of the catalytic cycle for ribonucleotide incorporation by the pol  $\lambda$  loop deletion variant provides insights into the distinct steps on the path for stable ribonucleotide incorporation.<sup>71</sup> In the precatalytic ternary complex structure, the incoming non-hydrolyzable analogue of an rNTP<sup>71</sup> occupies a position identical to that of an incoming dNTP in a corresponding precatalytic complex (Figure 7A,D). It is accommodated in the nucleotide-binding pocket without any distortion of the primer-terminal base pair or the active site. This is despite an unfavorable, short-range interaction (2.4 Å) between the 2'-OH on the ribose and the backbone carbonyl of Tyr505, which indicates an energetically unstable binding state for the rNTP. Consistent with this result, a study of sugar selection by pol  $\lambda$  suggested that the 2'-OH of the ribose is excluded mainly because of a steric clash with the segment of the backbone between Y505 and G508.<sup>84</sup> A similar unfavorable interaction with an incoming rNTP and a homologous tyrosine residue (Tyr271) has been described for pol  $\beta$ .<sup>85</sup> This is in contrast to polymerases from other families, which depend on bulky side chains for steric exclusion of the incorrect sugar.<sup>81</sup> The unfavorable binding state for the incoming rNTP appears to be stabilized by interactions of arginine side chains (Arg386 and Arg420) with the  $\beta$ - and  $\gamma$ -phosphates. Thus, the correct geometry at the active site is maintained, allowing for catalysis to occur upon substitution of the nonhydrolyzable nucleotide by a normal rNTP. However, unlike insertion of a dNTP, the breakage and formation of the new phosphorus–oxygen bond during incorporation of a ribonucleotide results in severe distortion of the postcatalytic product complex (Figure 7B,D). The 2'-OH on the sugar of the newly inserted dNMP is displaced from its precatalytic position and occupies the precatalytic position of the 3'-OH, causing the phosphate of the newly inserted nucleotide and the sugar of the preceding nucleotide to shift into the minor groove. Despite the distortion of the sugar–phosphate backbone, the base of the newly incorporated rNMP remains in its precatalytic position, forming the expected hydrogen bonds with its corresponding template nucleotide. Concurrently with the distortion of the primer strand, side chains Tyr505 and Phe506 revert to their inactive conformation. The distortion of the postcatalytic complex is

consistent with the unstable binding state for the incoming rNTP in the precatalytic complex and suggests that once the bond between the  $\alpha$ - and  $\beta$ -phosphate is broken, the energetically unstable binding state cannot be maintained.

It is not clear if and how this distortion affects translocation. However, upon translocation, when the rNMP is at the primer terminus, there is no distortion of the DNA or the protein (Figure 7C) and the primer-terminal rNMP does not hinder extension.<sup>71</sup> This suggests that pol  $\lambda$  could easily extend a ribonucleotide-terminated primer.

## ■ CONCLUDING REMARKS

The four mammalian family X members share common traits, but like pol  $\lambda$ , each has its own distinct features, including specific structural elements that define their functional properties. Although the exact cellular roles, including substrate specificities and specific protein partnerships, of family X members remain to be elucidated, their individual features and differences in behavior provide some clues about their *in vivo* functions. Future structural studies of pol  $\lambda$  and its siblings with substrates specific to each of their unique activities together with studies in cell-based systems and animal models should dramatically enhance our understanding of how these enzymes carry out their specific roles in DNA repair.

## ■ AUTHOR INFORMATION

### Corresponding Author

\*E-mail: bebenek@niehs.nih.gov. Phone: (919) 541-3535.

### Funding

Work in the laboratories of T.A.K. and L.C.P. is supported by the Division of Intramural Research of the National Institute of Environmental Health Sciences, National Institutes of Health, via Grants ES065070 and ES102645, respectively.

### Notes

The authors declare no competing financial interest.

## ■ ACKNOWLEDGMENTS

We thank Bill Beard and Andrea Moon for critical reading of the manuscript as well as the Ramsden and Blanco laboratories for helpful discussions and collaboration.

## ■ ABBREVIATIONS

pol, polymerase; DSBs, double-strand breaks; BER, base excision repair; NHEJ, nonhomologous end joining; TdT, terminal deoxynucleotidyl transferase; dRP lyase, deoxyribose phosphate lyase; 8-oxodG, 8-oxo-7,8-dihydro-2'-deoxyguanosine; BRCT, breast cancer susceptibility gene 1 C-terminal; TLS, translesion synthesis; dNTP, deoxyribonucleoside triphosphate; rNTP, ribonucleoside triphosphate; PDB, Protein Data Bank.

## ■ REFERENCES

- (1) Uchiyama, Y., Takeuchi, R., Kodera, H., and Sakaguchi, K. (2009) Distribution and roles of X-family DNA polymerases in eukaryotes. *Biochimie* 91, 165–170.
- (2) Oliveros, M., Yanez, R. J., Salas, M. L., Salas, J., Vinuela, E., and Blanco, L. (1997) Characterization of an African swine fever virus 20-kDa DNA polymerase involved in DNA repair. *J. Biol. Chem.* 272, 30899–30910.
- (3) Sobol, R. W., Horton, J. K., Kuhn, R., Gu, H., Singhal, R. K., Prasad, R., Rajewsky, K., and Wilson, S. H. (1996) Requirement of mammalian DNA polymerase- $\beta$  in base-excision repair. *Nature* 379, 183–186.

- (4) Garcia-Diaz, M., Bebenek, K., Kunkel, T. A., and Blanco, L. (2001) Identification of an intrinsic 5'-deoxyribose-5'-phosphate lyase activity in human DNA polymerase  $\lambda$ : A possible role in base excision repair. *J. Biol. Chem.* 276, 34659–34663.
- (5) Braithwaite, E. K., Kedar, P. S., Lan, L., Polosina, Y. Y., Asagoshi, K., Poltoratsky, V. P., Horton, J. K., Miller, H., Teebor, G. W., Yasui, A., and Wilson, S. H. (2005) DNA polymerase  $\lambda$  protects mouse fibroblasts against oxidative DNA damage and is recruited to sites of DNA damage/repair. *J. Biol. Chem.* 280, 31641–31647.
- (6) Braithwaite, E. K., Kedar, P. S., Stumpo, D. J., Bertocci, B., Freedman, J. H., Samson, L. D., and Wilson, S. H. (2010) DNA polymerases  $\beta$  and  $\lambda$  mediate overlapping and independent roles in base excision repair in mouse embryonic fibroblasts. *PLoS One* 5, e12229.
- (7) Brown, J. A., Duym, W. W., Fowler, J. D., and Suo, Z. (2007) Single-turnover kinetic analysis of the mutagenic potential of 8-oxo-7,8-dihydro-2'-deoxyguanosine during gap-filling synthesis catalyzed by human DNA polymerases  $\lambda$  and  $\beta$ . *J. Mol. Biol.* 367, 1258–1269.
- (8) Maga, G., Villani, G., Crespan, E., Wimmer, U., Ferrari, E., Bertocci, B., and Hubscher, U. (2007) 8-oxo-guanine bypass by human DNA polymerases in the presence of auxiliary proteins. *Nature* 447, 606–608.
- (9) van Loon, B., and Hubscher, U. (2009) An 8-oxo-guanine repair pathway coordinated by MUTYH glycosylase and DNA polymerase  $\lambda$ . *Proc. Natl. Acad. Sci. U.S.A.* 106, 18201–18206.
- (10) Pardo, B., Gomez-Gonzalez, B., and Aguilera, A. (2009) DNA repair in mammalian cells: DNA double-strand break repair: How to fix a broken relationship. *Cell. Mol. Life Sci.* 66, 1039–1056.
- (11) Suberbielle, E., Sanchez, P. E., Kravitz, A. V., Wang, X., Ho, K., Eilertson, K., Devidze, N., Kreitzer, A. C., and Mucke, L. (2013) Physiologic brain activity causes DNA double-strand breaks in neurons, with exacerbation by amyloid- $\beta$ . *Nat. Neurosci.* 16, 613–621.
- (12) Lieber, M. R., Ma, Y., Pannicke, U., and Schwarz, K. (2003) Mechanism and regulation of human non-homologous DNA end-joining. *Nat. Rev. Mol. Cell Biol.* 4, 712–720.
- (13) Ramsden, D. A., and Asagoshi, K. (2012) DNA polymerases in nonhomologous end joining: Are there any benefits to standing out from the crowd? *Environ. Mol. Mutagen.* 53, 741–751.
- (14) Chiruvella, K. K., Liang, Z., and Wilson, T. E. (2013) Repair of double-strand breaks by end joining. *Cold Spring Harbor Perspect. Biol.* 5, a012757.
- (15) Bertocci, B., De Smet, A., Weill, J. C., and Reynaud, C. A. (2006) Nonoverlapping functions of DNA polymerases  $\mu$ ,  $\lambda$ , and terminal deoxynucleotidyltransferase during immunoglobulin V(D)J recombination in vivo. *Immunity* 25, 31–41.
- (16) Bertocci, B., De Smet, A., Berek, C., Weill, J. C., and Reynaud, C. A. (2003) Immunoglobulin  $\kappa$  light chain gene rearrangement is impaired in mice deficient for DNA polymerase  $\mu$ . *Immunity* 19, 203–211.
- (17) Lee, J. W., Blanco, L., Zhou, T., Garcia-Diaz, M., Bebenek, K., Kunkel, T. A., Wang, Z., and Povirk, L. F. (2004) Implication of DNA polymerase  $\lambda$  in alignment-based gap filling for nonhomologous DNA end joining in human nuclear extracts. *J. Biol. Chem.* 279, 805–811.
- (18) Zhou, R. Z., Blanco, L., Garcia-Diaz, M., Bebenek, K., Kunkel, T. A., and Povirk, L. F. (2008) Tolerance for 8-oxoguanine but not thymine glycol in alignment-based gap filling of partially complementary double-strand break ends by DNA polymerase  $\lambda$  in human nuclear extracts. *Nucleic Acids Res.* 36, 2895–2905.
- (19) Ma, Y., Lu, H., Tippin, B., Goodman, M. F., Shimazaki, N., Koizumi, O., Hsieh, C. L., Schwarz, K., and Lieber, M. R. (2004) A biochemically defined system for mammalian nonhomologous DNA end joining. *Mol. Cell* 16, 701–713.
- (20) Nick McElhinny, S. A., Havener, J. M., Garcia-Diaz, M., Juarez, R., Bebenek, K., Kee, B. L., Blanco, L., Kunkel, T. A., and Ramsden, D. A. (2005) A gradient of template dependence defines distinct biological roles for family X polymerases in nonhomologous end joining. *Mol. Cell* 19, 357–366.
- (21) Ogiwara, H., and Kohno, T. (2011) Essential factors for incompatible DNA end joining at chromosomal DNA double strand breaks in vivo. *PLoS One* 6, e28756.
- (22) Waters, L. S., Minesinger, B. K., Wiltout, M. E., D'Souza, S., Woodruff, R. V., and Walker, G. C. (2009) Eukaryotic translesion polymerases and their roles and regulation in DNA damage tolerance. *Microbiol. Mol. Biol. Rev.* 73, 134–154.
- (23) Maga, G., Villani, G., Ramadan, K., Shevelev, I., Tanguy Le Gac, N., Blanco, L., Blanca, G., Spadari, S., and Hubscher, U. (2002) Human DNA polymerase  $\lambda$  functionally and physically interacts with proliferating cell nuclear antigen in normal and translesion DNA synthesis. *J. Biol. Chem.* 277, 48434–48440.
- (24) Blanca, G., Villani, G., Shevelev, I., Ramadan, K., Spadari, S., Hubscher, U., and Maga, G. (2004) Human DNA polymerases  $\lambda$  and  $\beta$  show different efficiencies of translesion DNA synthesis past abasic sites and alternative mechanisms for frameshift generation. *Biochemistry* 43, 11605–11615.
- (25) Maga, G., Crespan, E., Markkanen, E., Imhof, R., Furrer, A., Villani, G., Hubscher, U., and van Loon, B. (2013) DNA polymerase  $\delta$ -interacting protein 2 is a processivity factor for DNA polymerase  $\lambda$  during 8-oxo-7,8-dihydroguanine bypass. *Proc. Natl. Acad. Sci. U.S.A.* 110, 18850–18855.
- (26) Belousova, E. A., Maga, G., Fan, Y., Kubareva, E. A., Romanova, E. A., Lebedeva, N. A., Oretskaya, T. S., and Lavrik, O. I. (2010) DNA polymerases  $\beta$  and  $\lambda$  bypass thymine glycol in gapped DNA structures. *Biochemistry* 49, 4695–4704.
- (27) Skosareva, L. V., Lebedeva, N. A., Rechkunova, N. I., Kolbanovskiy, A., Geacintov, N. E., and Lavrik, O. I. (2012) Human DNA polymerase  $\lambda$  catalyzes lesion bypass across benzo[a]pyrene-derived DNA adduct during base excision repair. *DNA Repair* 11, 367–373.
- (28) Garcia-Diaz, M., Dominguez, O., Lopez-Fernandez, L. A., de Lera, L. T., Saniger, M. L., Ruiz, J. F., Parraga, M., Garcia-Ortiz, M. J., Kirchhoff, T., del Mazo, J., Bernad, A., and Blanco, L. (2000) DNA polymerase  $\lambda$  (Pol  $\lambda$ ), a novel eukaryotic DNA polymerase with a potential role in meiosis. *J. Mol. Biol.* 301, 851–867.
- (29) Aoufouchi, S., Flatter, E., Dahan, A., Faily, A., Bertocci, B., Storck, S., Delbos, F., Cocea, L., Gupta, N., Weill, J. C., and Reynaud, C. A. (2000) Two novel human and mouse DNA polymerases of the polX family. *Nucleic Acids Res.* 28, 3684–3693.
- (30) Nagasawa, K., Kitamura, K., Yasui, A., Nimura, Y., Ikeda, K., Hirai, M., Matsukage, A., and Nakanishi, M. (2000) Identification and characterization of human DNA polymerase  $\beta$ 2, a DNA polymerase  $\beta$ -related enzyme. *J. Biol. Chem.* 275, 31233–31238.
- (31) Bebenek, K., Garcia-Diaz, M., Blanco, L., and Kunkel, T. A. (2003) The frameshift infidelity of human DNA polymerase  $\lambda$ . Implications for function. *J. Biol. Chem.* 278, 34685–34690.
- (32) Garcia-Diaz, M., Bebenek, K., Sabariego, R., Dominguez, O., Rodriguez, J., Kirchhoff, T., Garcia-Palomero, E., Picher, A. J., Juarez, R., Ruiz, J. F., Kunkel, T. A., and Blanco, L. (2002) DNA polymerase  $\lambda$ , a novel DNA repair enzyme in human cells. *J. Biol. Chem.* 277, 13184–13191.
- (33) Garcia-Diaz, M., Bebenek, K., Krahn, J. M., Kunkel, T. A., and Pedersen, L. C. (2005) A closed conformation for the Pol  $\lambda$  catalytic cycle. *Nat. Struct. Mol. Biol.* 12, 97–98.
- (34) Sawaya, M. R., Prasad, R., Wilson, S. H., Kraut, J., and Pelletier, H. (1997) Crystal structures of human DNA polymerase  $\beta$  complexed with gapped and nicked DNA: Evidence for an induced fit mechanism. *Biochemistry* 36, 11205–11215.
- (35) Moon, A. F., Garcia-Diaz, M., Bebenek, K., Davis, B. J., Zhong, X., Ramsden, D. A., Kunkel, T. A., and Pedersen, L. C. (2007) Structural insight into the substrate specificity of DNA polymerase  $\mu$ . *Nat. Struct. Mol. Biol.* 14, 45–53.
- (36) Garcia-Diaz, M., Bebenek, K., Krahn, J. M., Blanco, L., Kunkel, T. A., and Pedersen, L. C. (2004) A structural solution for the DNA polymerase  $\lambda$ -dependent repair of DNA gaps with minimal homology. *Mol. Cell* 13, 561–572.
- (37) Tseng, H. M., and Tomkinson, A. E. (2002) A physical and functional interaction between yeast Pol4 and Dnl4-Lif1 links DNA

synthesis and ligation in nonhomologous end joining. *J. Biol. Chem.* 277, 45630–45637.

(38) Fan, W., and Wu, X. (2004) DNA polymerase  $\lambda$  can elongate on DNA substrates mimicking non-homologous end joining and interact with XRCC4-ligase IV complex. *Biochem. Biophys. Res. Commun.* 323, 1328–1333.

(39) Mahajan, K. N., Nick McElhinny, S. A., Mitchell, B. S., and Ramsden, D. A. (2002) Association of DNA polymerase  $\mu$  (pol  $\mu$ ) with Ku and ligase IV: Role for pol  $\mu$  in end-joining double-strand break repair. *Mol. Cell. Biol.* 22, 5194–5202.

(40) Mueller, G. A., Moon, A. F., Derose, E. F., Havener, J. M., Ramsden, D. A., Pedersen, L. C., and London, R. E. (2008) A comparison of BRCT domains involved in nonhomologous end-joining: Introducing the solution structure of the BRCT domain of polymerase lambda. *DNA Repair* 7, 1340–1351.

(41) DeRose, E. F., Clarkson, M. W., Gilmore, S. A., Galban, C. J., Tripathy, A., Havener, J. M., Mueller, G. A., Ramsden, D. A., London, R. E., and Lee, A. L. (2007) Solution structure of polymerase mu's BRCT domain reveals an element essential for its role in non-homologous end joining. *Biochemistry* 46, 12100–12110.

(42) Markkanen, E., van Loon, B., Ferrari, E., Parsons, J. L., Dianov, G. L., and Hubscher, U. (2012) Regulation of oxidative DNA damage repair by DNA polymerase  $\lambda$  and MutYH by cross-talk of phosphorylation and ubiquitination. *Proc. Natl. Acad. Sci. U.S.A.* 109, 437–442.

(43) Fiala, K. A., Duym, W. W., Zhang, J., and Suo, Z. (2006) Up-regulation of the fidelity of human DNA polymerase  $\lambda$  by its non-enzymatic proline-rich domain. *J. Biol. Chem.* 281, 19038–19044.

(44) Singhal, R. K., and Wilson, S. H. (1993) Short gap-filling synthesis by DNA polymerase  $\beta$  is processive. *J. Biol. Chem.* 268, 15906–15911.

(45) DeRose, E. F., Kirby, T. W., Mueller, G. A., Bebenek, K., Garcia-Diaz, M., Blanco, L., Kunkel, T. A., and London, R. E. (2003) Solution structure of the lyase domain of human DNA polymerase  $\lambda$ . *Biochemistry* 42, 9564–9574.

(46) Martin, M. J., Garcia-Ortiz, M. V., Gomez-Bedoya, A., Esteban, V., Guerra, S., and Blanco, L. (2013) A specific N-terminal extension of the 8 kDa domain is required for DNA end-bridging by human Pol  $\mu$  and Pol  $\lambda$ . *Nucleic Acids Res.* 41, 9105–9116.

(47) Joyce, C. M., and Steitz, T. A. (1995) Polymerase structures and function: Variations on a theme? *J. Bacteriol.* 177, 6321–6329.

(48) Joyce, C. M., and Benkovic, S. J. (2004) DNA polymerase fidelity: Kinetics, structure, and checkpoints. *Biochemistry* 43, 14317–14324.

(49) Doublet, S., Sawaya, M. R., and Ellenberger, T. (1999) An open and closed case for all polymerases. *Structure* 7, R31–R35.

(50) Li, Y., Korolev, S., and Waksman, G. (1998) Crystal structures of open and closed forms of binary and ternary complexes of the large fragment of *Thermus aquaticus* DNA polymerase I: Structural basis for nucleotide incorporation. *EMBO J.* 17, 7514–7525.

(51) Kunkel, T. A., and Bebenek, K. (2000) DNA replication fidelity. *Annu. Rev. Biochem.* 69, 497–529.

(52) Garcia-Diaz, M., Bebenek, K., Krahn, J. M., Pedersen, L. C., and Kunkel, T. A. (2007) Role of the catalytic metal during polymerization by DNA polymerase  $\lambda$ . *DNA Repair* 6, 1333–1340.

(53) Cisneros, G. A., Perera, L., Garcia-Diaz, M., Bebenek, K., Kunkel, T. A., and Pedersen, L. G. (2008) Catalytic mechanism of human DNA polymerase  $\lambda$  with  $Mg^{2+}$  and  $Mn^{2+}$  from ab initio quantum mechanical/molecular mechanical studies. *DNA Repair* 7, 1824–1834.

(54) Steitz, T. A. (1999) DNA polymerases: Structural diversity and common mechanisms. *J. Biol. Chem.* 274, 17395–17398.

(55) Blanca, G., Shevelev, I., Ramadan, K., Villani, G., Spadari, S., Hubscher, U., and Maga, G. (2003) Human DNA polymerase  $\lambda$  diverged in evolution from DNA polymerase  $\beta$  toward specific  $Mn^{2+}$  dependence: A kinetic and thermodynamic study. *Biochemistry* 42, 7467–7476.

(56) Nakamura, T., Zhao, Y., Yamagata, Y., Hua, Y. J., and Yang, W. (2012) Watching DNA polymerase  $\eta$  make a phosphodiester bond. *Nature* 487, 196–201.

(57) Freudenthal, B. D., Beard, W. A., Shock, D. D., and Wilson, S. H. (2013) Observing a DNA polymerase choose right from wrong. *Cell* 154, 157–168.

(58) Beard, W. A., and Wilson, S. H. (2014) Structure and mechanism of DNA polymerase  $\beta$ . *Biochemistry* 53, DOI: 10.1021/bi500139h.

(59) Yang, W. (2014) A summary of Y-family DNA polymerases and a case study of human polymerase  $\eta$ . *Biochemistry* 53, DOI: 10.1021/bi500019s.

(60) Batra, V. K., Beard, W. A., Shock, D. D., Krahn, J. M., Pedersen, L. C., and Wilson, S. H. (2006) Magnesium-induced assembly of a complete DNA polymerase catalytic complex. *Structure* 14, 757–766.

(61) Garcia-Diaz, M., Bebenek, K., Larrea, A. A., Havener, J. M., Perera, L., Krahn, J. M., Pedersen, L. C., Ramsden, D. A., and Kunkel, T. A. (2009) Template strand scrunching during DNA gap repair synthesis by human polymerase  $\lambda$ . *Nat. Struct. Mol. Biol.* 16, 967–972.

(62) Garcia-Diaz, M., and Kunkel, T. A. (2006) Mechanism of a genetic glissando: Structural biology of indel mutations. *Trends Biochem. Sci.* 31, 206–214.

(63) Bebenek, K., and Kunkel, T. A. (2000) Streisinger revisited: DNA synthesis errors mediated by substrate misalignments. *Cold Spring Harbor Symp. Quant. Biol.* 65, 81–91.

(64) Kunkel, T. A. (2004) DNA replication fidelity. *J. Biol. Chem.* 279, 16895–16898.

(65) Streisinger, G., et al. (1966) Frameshift mutations and the genetic code. *Cold Spring Harbor Symp. Quant. Biol.* 31, 77–84.

(66) Streisinger, G., and Owen, J. (1985) Mechanisms of spontaneous and induced frameshift mutation in bacteriophage T4. *Genetics* 109, 633–659.

(67) Garcia-Diaz, M., Bebenek, K., Krahn, J. M., Pedersen, L. C., and Kunkel, T. A. (2006) Structural analysis of strand misalignment during DNA synthesis by a human DNA polymerase. *Cell* 124, 331–342.

(68) Estabrook, R. A., Lipson, R., Hopkins, B., and Reich, N. (2004) The coupling of tight DNA binding and base flipping: Identification of a conserved structural motif in base flipping enzymes. *J. Biol. Chem.* 279, 31419–31428.

(69) Slupphaug, G., Mol, C. D., Kavli, B., Arvai, A. S., Krokan, H. E., and Tainer, J. A. (1996) A nucleotide-flipping mechanism from the structure of human uracil-DNA glycosylase bound to DNA. *Nature* 384, 87–92.

(70) Bebenek, K., Garcia-Diaz, M., Zhou, R. Z., Povirk, L. F., and Kunkel, T. A. (2010) Loop 1 modulates the fidelity of DNA polymerase  $\lambda$ . *Nucleic Acids Res.* 38, 5419–5431.

(71) Gosavi, R. A., Moon, A. F., Kunkel, T. A., Pedersen, L. C., and Bebenek, K. (2012) The catalytic cycle for ribonucleotide incorporation by human DNA Pol  $\lambda$ . *Nucleic Acids Res.* 40, 7518–7527.

(72) Bebenek, K., Pedersen, L. C., and Kunkel, T. A. (2011) Replication infidelity via a mismatch with Watson-Crick geometry. *Proc. Natl. Acad. Sci. U.S.A.* 108, 1862–1867.

(73) Watson, J. D., and Crick, F. H. C. (1953) A structure for deoxyribose nucleic acid. *Nature* 171, 737–738.

(74) Drake, J. W., and Baltz, R. H. (1976) The biochemistry of mutagenesis. *Annu. Rev. Biochem.* 45, 11–37.

(75) Wang, W., Hellinga, H. W., and Beese, L. S. (2011) Structural evidence for the rare tautomer hypothesis of spontaneous mutagenesis. *Proc. Natl. Acad. Sci. U.S.A.* 108, 17644–17648.

(76) Nick McElhinny, S. A., Watts, B. E., Kumar, D., Watt, D. L., Lundstrom, E. B., Burgers, P. M., Johansson, E., Chabes, A., and Kunkel, T. A. (2010) Abundant ribonucleotide incorporation into DNA by yeast replicative polymerases. *Proc. Natl. Acad. Sci. U.S.A.* 107, 4949–4954.

(77) Nick McElhinny, S. A., Kumar, D., Clark, A. B., Watt, D. L., Watts, B. E., Lundstrom, E. B., Johansson, E., Chabes, A., and Kunkel, T. A. (2010) Genome instability due to ribonucleotide incorporation into DNA. *Nat. Chem. Biol.* 6, 774–781.

(78) Boule, J. B., Rougeon, F., and Papanicolaou, C. (2001) Terminal deoxynucleotidyl transferase indiscriminately incorporates ribonucleotides and deoxyribonucleotides. *J. Biol. Chem.* 276, 31388–31393.

(79) Nick McElhinny, S. A., and Ramsden, D. A. (2003) Polymerase  $\mu$  is a DNA-directed DNA/RNA polymerase. *Mol. Cell. Biol.* 23, 2309–2315.

(80) Ruiz, J. F., Juarez, R., Garcia-Diaz, M., Terrados, G., Picher, A. J., Gonzalez-Barrera, S., Fernandez de Henestrosa, A. R., and Blanco, L. (2003) Lack of sugar discrimination by human Pol  $\mu$  requires a single glycine residue. *Nucleic Acids Res.* 31, 4441–4449.

(81) Brown, J. A., and Suo, Z. (2011) Unlocking the sugar “steric gate” of DNA polymerases. *Biochemistry* 50, 1135–1142.

(82) Cavanaugh, N. A., Beard, W. A., and Wilson, S. H. (2010) DNA polymerase  $\beta$  ribonucleotide discrimination: Insertion, misinsertion, extension, and coding. *J. Biol. Chem.* 285, 24457–24465.

(83) Martin, M. J., Garcia-Ortiz, M. V., Esteban, V., and Blanco, L. (2013) Ribonucleotides and manganese ions improve non-homologous end joining by human Pol  $\mu$ . *Nucleic Acids Res.* 41, 2428–2436.

(84) Brown, J. A., Fiala, K. A., Fowler, J. D., Sherrer, S. M., Newmister, S. A., Duym, W. W., and Suo, Z. (2010) A novel mechanism of sugar selection utilized by a human X-family DNA polymerase. *J. Mol. Biol.* 395, 282–290.

(85) Cavanaugh, N. A., Beard, W. A., Batra, V. K., Perera, L., Pedersen, L. G., and Wilson, S. H. (2011) Molecular insights into DNA polymerase deterrents for ribonucleotide insertion. *J. Biol. Chem.* 286, 31650–31660.

(86) Brown, J. A., Pack, L. R., Sanman, L. E., and Suo, Z. (2011) Efficiency and fidelity of human DNA polymerases  $\lambda$  and  $\beta$  during gap-filling DNA synthesis. *DNA Repair* 10, 24–33.